Article

In Situ Electrochemical Monitoring of Caged Compound Photochemistry: An Internal Actinometer for Substrate Release

Romana Jarosova, Sam V. Kaplan, Thomas M. Field, Richard S. Givens, Sanjeewa N. Senadheera, and Michael A. Johnson*

ACCESS | Metrics & More | Article Recommendations

ABSTRACT: Caged compounds are molecules that release a protective substrate to free a biologically active substrate upon treatment with light of sufficient energy and duration. A notable limitation of this approach is difficulty in determining the degree of photoactivation in tissues or opaque solutions because light reaching the desired location is obstructed. Here, we have addressed this issue by developing an *in situ* electrochemical method in which the amount of caged molecule photorelease is determined by fast-scan cyclic voltammetry (FSCV) at carbon-fiber microelectrodes. Using *p*-hydroxyphenyl glutamate (*p*HP-Glu) as our model system, we generated a linear calibration curve for oxidation of 4-hydroxyphenylacetic acid (4HPAA), the group from which the glutamate molecule leaves, up to a concentration of 1000 μM. Moreover, we are able to correct for the presence of residual *p*HP-Glu in solution as well as the light artifact that is produced. A corrected calibration curve was constructed by photoactivation of *p*HP-Glu in a 3 μL photoreaction vessel and subsequent analysis by high-performance liquid chromatography. This approach has yielded a linear relationship between 4HPAA concentration and oxidation current, allowing the determination of released glutamate independent of the amount of light reaching the chromophore. Moreover, we have successfully validated the newly developed method by *in situ* measurement in a whole, intact zebrafish brain. This work demonstrates for the first time the *in situ* electrochemical monitoring of caged compound photochemistry in brain tissue with FSCV, thus facilitating analyses of neuronal function.
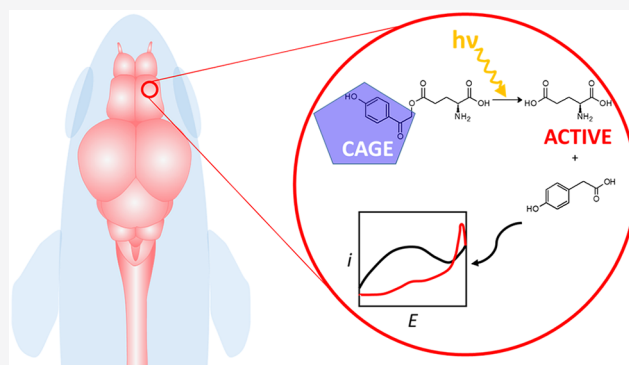
The use of light-driven approaches to manipulate biological systems has grown dramatically over the past decade. One such approach, caged compound photoactivation, allows the application of biologically active molecules with micrometer spatial and sub-second temporal resolution. When treated with light of sufficient energy, the photoremovable protecting group on a caged compound separates from the biologically active form of the molecule.[1−6] This photochemical delivery method has been used to activate biologically dormant or inactive biosystems such as neurons and sensory cells in *ex vivo* and *in vivo* tissue platforms as well as reactions at the molecular level such as enzymatic reactions and protein folding. Moreover, the protecting group's rapid release occurs within nanoseconds (ns) to microseconds (μs) depending on the protecting group and the substrate,[7] making this photoactivation process compatible for probing temporal and spatial parameters by electrophysiological and electrochemical detection methods. For example, caged substrate photoactivation combines the photorelease process with patch clamp detection to examine the influence of the amino acids glutamate and γ-aminobutyric acid (GABA) as agonists and antagonists for neuronal function.[2,3,5,8−13] The function of dopaminergic neurons and circuits can be explored using recently developed caged dopamine and its caged receptor antagonists.[14,15]

A major challenge of this approach, as well as others that employ photoactivation strategies, is quantitation of a photoreleased substrate when sample variability is not controlled. Traditionally, the amount of a photoreleased substrate has been determined indirectly by measuring the photon flux impinging on the sample using actinometry methods, e.g., potassium ferrioxalate solutions[16] and the quantum yield (the ratio of yield to photons absorbed) for substrate release upon exposure to the light source. By

knowing the quantum yield, one can determine the number of moles released when the number of photons absorbed by the sample is known. This approach is reliable as long as the photon delivery system and the substrate photolysis reaction are identical for both the actinometry and substrate release measurements.

Determination of yields of the photoreleased substrate in complex biological and tissue entrainments present additional confounding variables. Such complications arise because actinometer solutions are homogeneous and contain only the reactive chromophore in physiological media. Conversely, in actual physiological experiments, there may be several competing chromophores as well as opaque materials that competitively absorb light or reflect it away from the caged material. This interference diminishes the amount of light reaching the caged compound, thereby resulting in an overestimation of substrate release.

A direct, *in situ* measurement of photorelease of the substrate, which is independent of interferences of the incident light and the nature of the biological sample, would mitigate many of the inherent complications associated with traditional actinometer methods. We propose a remedy for quantifying the photoreaction by employing a doubly responsive photoreaction that couples substrate release with the generation of a separate electroactive byproduct. This concept parallels the photogeneration of active fluorophores with substrate release that uses fluorescence intensities to quantify the release.[3]

Fast-scan cyclic voltammetry (FSCV) is a technique of choice for measuring chemicals secreted from individual cells,[16,17] in acutely dissociated brain sections,[12,16,18−22] and in whole animals.[23−28] This method is compatible with caged compound photoactivation studies because it has good temporal resolution (sub-second to millisecond), selectivity (a characteristic cyclic voltammogram, or CV, is formed), and spatial resolution (nanometer to micrometer). Here, we report a new synergistic approach by FSCV to quantify photoactivation of substrate release and caged compound decomposition simultaneously with an *in situ* single probe. The concept requires that the byproduct of the caging chromophore be electroactive, but preferably not the caged compound itself. However, as demonstrated here, the starting material signal can be subtracted to remove it from interfering with the product analyses.

In this work, we use a *p*-hydroxyphenacyl cage to demonstrate proof of concept for the electrochemical monitoring of photoactivation. The use of this cage for a wide variety of substrates has several inherent advantages for FSCV-based analyses. The *p*HP class of caged compounds offers high quantum yields, nanosecond timescales of release, and deep-seated rearrangement of the caging chromophore into biologically benign 4-hydroxyphenylacetic acid (4HPAA; Figure 1). This molecule can be measured electrochemically and distinguished from other biologically active compounds such as monoamine neurotransmitters.[29]

The method described here uses a microliter photoreaction vessel to generate a calibration curve that relates the electrochemical oxidation signal of photoreleased 4HPAA measured by FSCV to the concentration of 4HPAA obtained by HPLC with ultraviolet−visible detection. We have previously demonstrated the simultaneous, electrochemical quantitation of 4HPAA *vs* dopamine by FSCV.[30] Thus, the method proposed here extends our capability to include the
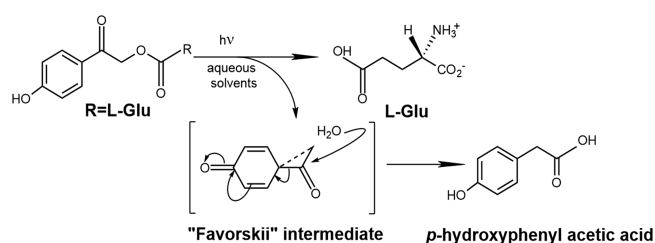

Figure 1. Reaction mechanism of uncaging *p*-hydroxyphenacyl-based compounds.

direct measurement of caged compound degradation in conjunction with dopamine release.

EXPERIMENTAL SECTION

Reagents. A stock solution (0.1 mmol L^{-1}) of 4HPAA (CAS no. 156-38-7, 98%, Sigma-Aldrich, St Louis, MO) and *p*HP-Glu (synthesized by the Synthetic Chemical Biology Core of the Center for the Molecular Analysis of Disease Pathways at The University of Kansas, Lawrence) were prepared by dissolving the appropriate analyte mass in artificial cerebrospinal fluid (aCSF). The aCSF consisted of 126 mM NaCl, 2.5 mM KCl, 1.2 mM NaH_2PO_4, 2.4 mM $CaCl_2$, 1.2 mM $MgCl_2$, 25 mM $NaHCO_3$, and 20 mM HEPES, adjusted to a pH of 7.4. Solutions used for generating the calibration curves were prepared by serial dilution of the stock solution. A stock solution of 4HPAA was refrigerated in glass vials in the dark when not in use. A stock solution of *p*HP-Glu was prepared daily. All chemicals for high-performance liquid chromatography (HPLC) were obtained from Sigma-Aldrich (St Louis, MO). Ultrapure water (~18.2 MOhm-cm) was used to prepare all aqueous solutions.

Animals. Adult *Danio rerio* (zebrafish, AB wild-type strain) were purchased from Zebrafish International Resource Center (ZIRC, University of Oregon, Eugene, OR) and housed in the Shankel Structural Biology Center at the University of Kansas. The animals were housed in three-liter tanks (15−20 fish per three-liter system rack tank) that were connected to a recirculation filtration system. All tanks were maintained under constant chemical, biological, and mechanical filtration, as well as the UV sterilizing unit to ensure adequate conditions. Conductivity (~800 μS cm^{-1}) and pH (7.2) of the reverse osmosis purified system water (maintained at 28 °C) was controlled and adjusted using a Multiparameter Monitoring and Control Instrument 5200A (YSI, Yellow Springs, OH). Fish were fed twice a day and kept in a light/dark cycle (16 h/ 8 h). All procedures involving zebrafish were approved by the Animal Care and Use Committee of the University of Kansas.

Uncaging Apparatus. The experimental uncaging apparatus was adapted from an approach used previously for electrophysiology.[31] The output from a mercury lamp, directed through a 280 nm cut-off high-pass filter and gated with a shutter, was delivered to the sample through a fiber-optic cable (PolyMicro Technologies, Inc., Phoenix, AZ). A micromanipulator was used to position the fiber-optic cable near the carbon-fiber microelectrode.

Fast-Scan Cyclic Voltammetry. A ChemClamp potentiostat (Dagan, Minneapolis, MN, USA), modified to enhance the range of available gain settings, was used. Data were collected and analyzed using TarHeel CV software (R.M. Wightman and M.L.A.V. Heien, University of North Carolina, Chapel Hill, NC, USA). Carbon-fiber working electrodes were constructed

using previously published methods[25] and were trimmed to an exposed length of 40 μm. Electrodes were used in the flow injection analysis apparatus, the microliter reaction vessel, and in whole zebrafish brains. Flow injection analysis was carried out by directing the solution flow with a six-port sample injector through a custom designed flow cell. For the detection of 4HPAA, a triangular waveform was used in which potential (*vs* Ag/AgCl electrode) was linearly scanned from −0.4 V to +1.3 V to −0.4 V. The potential between scans was held at −0.4 V. The scan rate was 600 V/s and the update rate was 10 Hz.[30]

Electrochemical Measurement of *p*HP-Glutamate Photoactivation. A microliter reaction vessel (Figure 2)
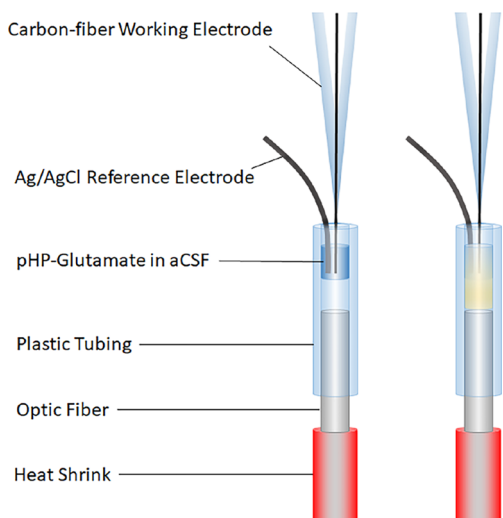

Figure 2. Microliter-scale reaction vessel used to determine the degree of photo-uncaging with FSCV. Left, without light application, and right, with light application through the optical fiber.

was fabricated with 1 mm plastic tubing (Cole Parmer, Vernon Hills, Illinois) that allowed a 3 μL volume of aqueous *p*HP-glutamate solution to be held in place by surface tension. A 1 mm diameter optical fiber (Polymicro Technologies, Phoenix, Arizona) was press fitted into the plastic tubing from the

bottom of the tubing, while the *p*Hp-glutamate solution was injected from the top of the tubing. The carbon-fiber working electrode and a Ag/AgCl reference electrode were micro-manipulated into the solution from the top of the reaction vessel. Once the photo-uncaging occurred and the photo-released 4HPAA was measured by FSCV, the electrodes were removed, and the sample was carefully transferred from the reaction vessel to a vial for a further HPLC analysis. To ensure sufficient amount of material for an HPLC analysis, three uncaging samples (*i.e.*, 3 × 3 μL) were consolidated into a vial for an HPLC analysis for each of the three electrodes. Measurements performed to quantify the photoelectric effect that were carried out in solutions in which *p*HP-Glu was not present.

Electrochemical Detection of *p*HP-Glutamate Photo-activation in a Zebrafish Brain. Zebrafish were euthanized by hypothermic shock followed by decapitation. Whole brains were harvested as described previously.[32] Briefly, the decapitated zebrafish head was immobilized in a Petri dish filled with 2% agarose (BioReagent grade, Sigma-Aldrich, St. Louis, MO, USA) and oxygenated (95% O_2 and 5% CO_2) aCSF. After removal from the skull, the fish brain was carefully lifted and transferred to a perfusion chamber. The brain was kept viable by a continuous flow of oxygenated aCSF heated at a physiological temperature of 28 °C. Prior to any measurement, the fish brain was first kept in the perfusion chamber for 40 min to equilibrate. The carbon-fiber working electrode was positioned into the ventral telencephalon of the zebrafish with a micropositioner. A 50 μm optic fiber (Polymicro Technologies, Phoenix, Arizona) was further micromanipu-lated into a close proximity of the tip of the carbon-fiber microelectrode. The photoelectric effect was examined in a zebrafish brain perfused by only aCSF (no *p*HP-glutamate presented). Finally, the *p*Hp-glutamate ($c = 1000$ μM) in aCSF was perfused through the brain for 30 min and the electrochemical detection of *p*HP-glutamate (4HPAA, respec-tively) was carried out. Both the photoelectric effect and the uncaging of *p*HP-glutamate in a zebrafish brain were performed using 1000 ms duration of light exposure.

HPLC Analysis. An HPLC system (Shimadzu Scientific Corp) is consisted of a CBA-20A system controller, a DGV-
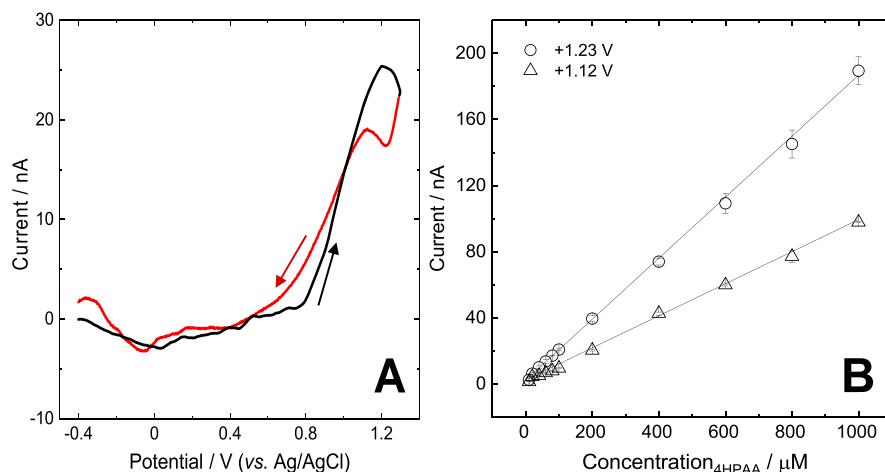

Figure 3. (A) Fast-scan cyclic voltammetric *i−E* curve for 100 μM 4HPAA in aCSF measured at a carbon-fiber microelectrode in flow injection arrangement. Two oxidation peaks occur at 1.23 and 1.12 V on the forward and backward sweep, respectively. Direction of the forward (black) and the reverse (red) potential sweep is indicated by arrows. (B) Response curves for 4HPAA in aCSF for injected concentrations from 10 to 1000 μM. Currents were evaluated at +1.23 V, open circles (○), and + 1.12 V , open triangles (△). Data are presented as mean ± std. dev. (N = 3).

20A3 degassing unit, an LC-20 AD high pressure pump, an SIL-20 AC autosampler, and an SDP-20 AV UV−Vis detector. An Ascentis C18 (15 cm × 4.6 mm × 5 μm) column (Millipore-Sigma, Inc., Burlington, MA) was used. The sample volume injected was 5 μL. The mobile phase consisted of (A) 99% H_2O, 1% MeOH, and 0.06% formic acid and (B) 99% MeOH, 1% H_2O, and 0.06% formic acid. Analytes were eluted isocratically at A:B = 70:30 (v/v %) at a flow rate of 1 mL min^{-1}. The spectrophotometric detector was set at 220 nm. The quantification of 4HPAA was performed by generation of an external calibration curve. The calibration curve was constructed from the height of the peak, as a function of 4HPAA concentration, with a linear dynamic range from 1 to 1000 μM ($R^2 = 0.9996$, N = 3).

Statistics. Statistical analysis and graphical presentation were carried out using OriginPro software, version 2020b (OriginLab Corp., Northampton, MA). A p-value of 0.05 or less was considered as significant.

■ RESULTS AND DISCUSSION

Measuring 4HPAA with FSCV. We have previously shown that 4HPAA can readily be measured by FSCV.[30] Thus, we sought here to demonstrate that the liberation of 4HPAA from p-hydroxyphenacyl-based caged compounds, such as p-hydroxyphenacyl glutamate, could be used to quantify the formation of the resulting bioactive molecule. Our approach quantifies glutamate photorelease by measuring differences between currents produced by the liberation of 4HPAA after light application and currents present prior to light application. Therefore, it is essential that the current associated with 4HPAA increase linearly within a useful concentration range. Figure 3A shows a CV of 4HPAA (0.1 mM) obtained by flow injection analysis and FSCV. As described by Shin et al.,[30] we observed two well-resolved peaks, suggesting that two distinct electrochemical processes occur. The first peak occurred at +1.23 V as the potential swept toward the most positive value, while the second peak occurred at +1.12 V as the potential swept toward the most negative value. Figure 3B shows that the electrochemical response to 4HPAA, evaluated from peaks at +1.23 V (forward sweep) and +1.12 V (backward sweep), was linear from 10 μM up to at least 1000 μM (higher concentrations were not investigated). This result indicates that it is possible to quantify the amount of 4HPAA photoreleased even at high concentrations.

Another concern was that the electroactivity of the caged form of the compound would complicate the interpretation of the electrochemical data because the CV is similar to that of 4HPAA. Despite the similarities, however, it is still possible to distinguish between the two voltammograms. For example, shown in Figure 4 are CVs of 4HPAA and pHP-Glu, obtained by flow injection analysis. The red trace is the result of subtracting the CV of pHP-Glu from that of 4HPAA. These CVs are unfolded at a switching potential of +1.3 V so that the direction of the potential sweep, which occurs from left to right in the figure, is easier to visualize. The oxidation peak for pHP-Glu appears at a similar position compared to the first oxidation peak of 4HPAA (about +1.23 V on the forward scan) and a small second pHP-Glu oxidation peak appears at +1.05 V on the backward scan. As the subtraction of the CVs reveals, a measurable signal proportional to the amount of 4HPAA formed by photo-uncaging can be derived by subtracting the two CVs. Even though in an actual uncaging experiment the
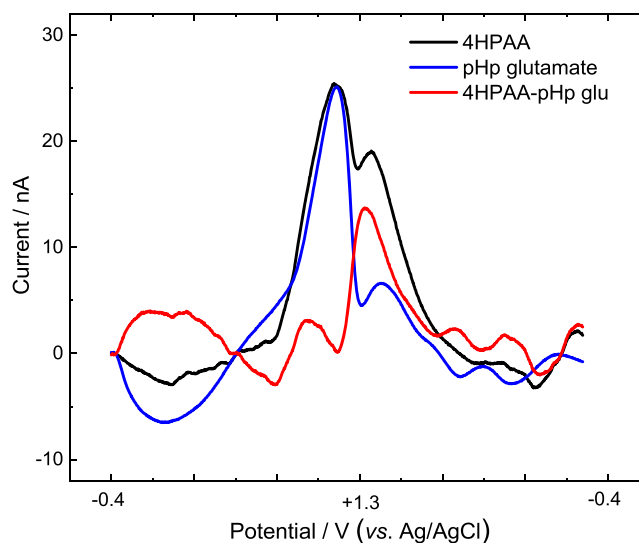

Figure 4. Flow injection analysis of pHP-Glu and 4HPAA. Solutions of 100 μM pHP-Glu and 100 μM 4HPAA in aCSF were injected separately. Parameters: scan rate, 600 V/s, update rate, 10 CVs/s, holding potential, −0.4 V.

concentrations of 4HPAA and pHP-Glu may not be equal due to the formation of species other than 4HPAA, the measurements in Figure 4 demonstrate that the CVs for the two species are qualitatively different and result in a characteristic CV upon subtraction.

Removing the Artifactual Light Signal from the 4HPAA Signal. Currents produced by photons striking the surface of the carbon-fiber microelectrode complicate the measurement of the current produced by 4HPAA because the CVs are similar. Therefore, we explored the effects of subtracting this signal from the overall electrochemical signal produced by photoactivation of pHP-Glu. Samples of aCSF with different concentrations of pHP-Glu, ranging from 0 to 1000 μM, were placed in the reaction vessel described in Figure 2. The solutions were exposed to light, gated by a shutter of selected durations ranging from 200 to 1000 ms. Even in the absence of pHP-Glu, the application of light produced a large photoinduced current that gradually decayed (Figure 5). The current response appeared to increase in linear fashion with increasing exposure time up to about 600 ms (Figure 6A). Beyond this time, the current deviated from linearity. Measurements obtained in the presence of successively increasing concentrations of pHP-Glu resulted in stepwise increase in measured current for all examined solutions (concentration of pHP-Glu from 400 to 1000 μM). The curvature similar to that found in the absence of pHP-Glu was evident in measurements obtained with successively increasing concentrations of pHP-Glu present in the solution; however, increasing the concentration tended to remove the curvature, particularly above concentrations of 600 μM.

The generation of currents upon exposure of electrode surfaces to visible and ultraviolet light has been documented.[33,34] Although these currents reach peak values over extended continuous exposure times, their measurement at carbon-fiber microelectrodes with FSCV has not been published in the literature, to our knowledge. We found that, in our particular case, this photoinduced current could be subtracted from the currents produced in the presence of pHP-Glu to yield current time points that fall into a linear
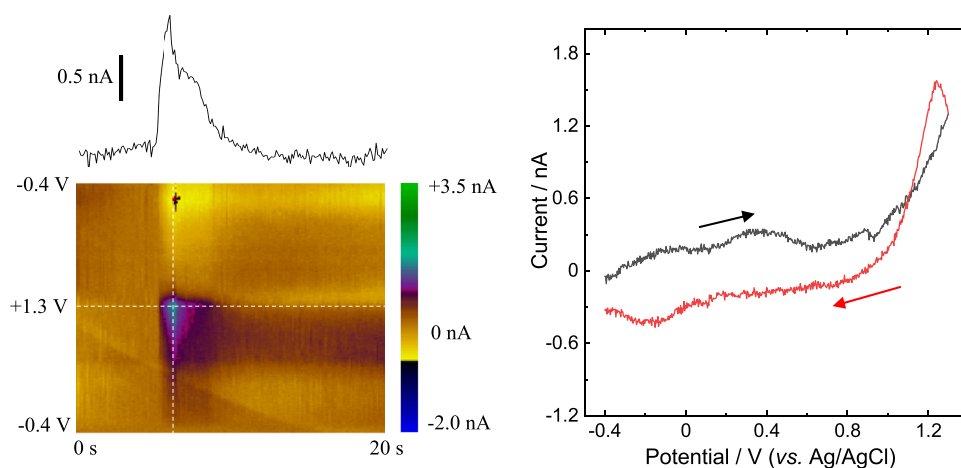
Figure 5. Current response measured in a solution containing 0 μM of *p*HP-Glu, and therefore, attributed to a light artifact. A representative current *vs* time plot (top), color plot (bottom), and FSCV (right) are shown. Direction of the potential sweep is indicated by arrows. Duration of light exposure: 1000 ms.
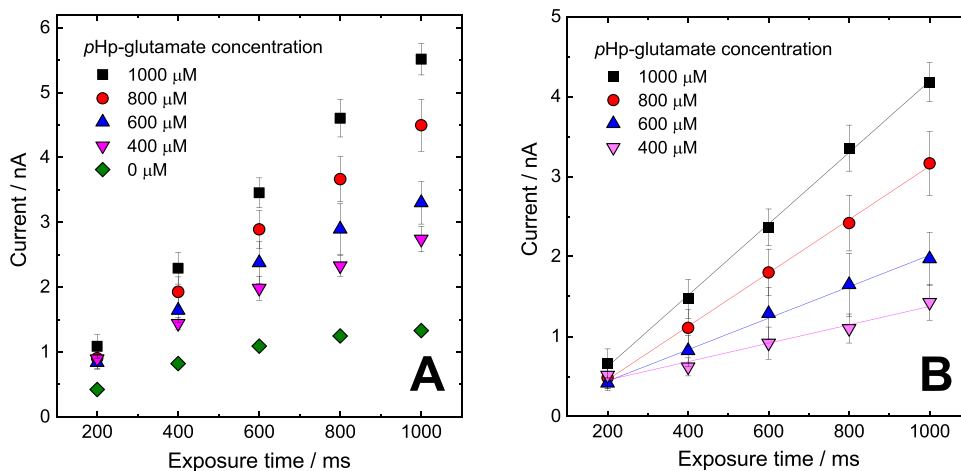

Figure 6. Light artifact removal. (A) Plot of the oxidation current *vs* the duration of light exposure. (B) Current response after the subtraction of the light artifact. Data are presented for three measurements at three different carbon-fiber microelectrodes as mean ± std. dev.

relationship with increasing time of light exposure (Figure 6B; linear regression analysis: R^2 = 0.9998 (1000 μM), 0.9987 (800 μM), 0.9942 (600 μM), and 0.9690 (400 μM), N = 3 electrodes). The linear character of these curves suggests that the light artifact can be removed from the overall electrochemical signal and the remaining currents can be used to monitor the formation of 4HPAA.

Generation of a Calibration Curve. Our ability to isolate currents produced by photolysis indicates that quantitation of 4HPAA in the solution is feasible. However, a critical aspect of this quantitation is the correction for other electrochemically active species present. Therefore, we designed a microliter reaction vessel (Figure 2) that allows direct comparison between oxidation currents that occur during photoreaction, obtained by FSCV, and the actual concentration of 4HPAA photoreleased, determined by high-performance liquid chromatography (HPLC). The reaction vessel was fabricated with an ~3 cm long segment of plastic tubing that allowed small volumes (~3 μL) of *p*HP-glutamate solution to be immobilized due to the surface tension of water. A 1 mm fiber-optic cable was positioned in the tube, but below the solution, so that the entire solution could be irradiated. After adding the solution, the carbon-fiber and Ag/AgCl electrodes

were inserted, thereby allowing the measurement of photo-uncaging events with electrochemistry.

We measured how 4HPAA concentration changes at different UV exposure times by combining FSCV and HPLC analyses. The process of generating a light intensity independent calibration curve is illustrated in Figures 7A−C. The typical recording of a photo-uncaging measurement involved the background subtraction of an averaged group of reference CVs, collected prior to light application, from the entire set of CVs obtained in the file. This operation removes current contributions from un-photolyzed *p*HP-Glu and generates a CV similar to that shown in Figure 4. The photo-uncaging of *p*HP-Glu, present in the vessel at an initial concentration of 1000 μM, was measured with FSCV as a function of exposure time. After removing the electrodes, the sample solution was analyzed by HPLC. Currents generated at each time point were also obtained in the absence of *p*HP-Glu and were subtracted from the measurements in which *p*HP-Glu was present. This operation removes the artifactual current generated by light application, similar to the subtraction process in Figure 6.

From this analysis, we constructed two linear graphs that plotted current (Figure 7A, R^2 = 0.9985) and 4HPAA
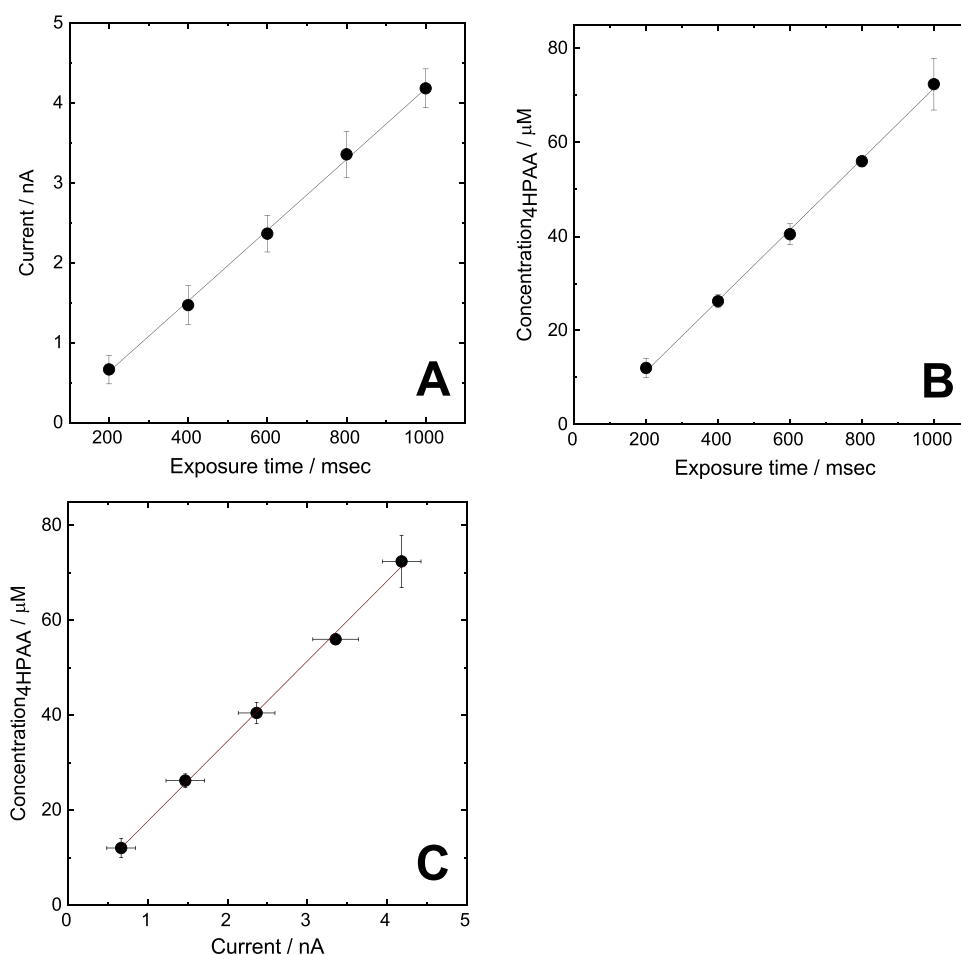
Figure 7. Generation of a calibration curve independent of the light source characteristics for an electrode. (A) Light artifact-subtracted current response (for 1000 μM pHP-glutamate) vs duration of light exposure. (B) Concentration of photoreleased 4HPAA determined via HPLC vs duration of light exposure. (C) Calibration curve obtained by combining (A, B). Data are reported as mean $\pm$ std. dev for $N = 3$ separate electrodes.

concentration (Figure 7B, R^2 = 0.9986) against exposure time. Combining these graphs provided a third linear plot that directly related current to 4HPAA concentration (Figure 7C, R^2 = 0.9980). By direct quantification of 4HPAA and knowing that 0.95 molecules of 4HPAA are released for every molecule of glutamate in aqueous solutions at physiological pH,[35,36] we are able to quantify glutamate generated by photoactivation of pHP-Glu. Therefore, this method represents the means for quantifying the released, biologically active glutamate that is more direct than actinometry. Furthermore, knowing the relative yield and the quantum efficiency for 4HPAA from the photorelease of any pHP leaving group (whether electroactive or not), one can temporally track the concentration of the leaving group on a real-time basis in a microliter-sized vessel.

Electrochemical Detection of pHP-Glutamate Photoactivation in a Zebrafish Brain. We next sought to validate our newly developed method for *in situ* electrochemical detection of photoreleased 4HPAA in a living, whole zebrafish brain, which is opaque. After brain dissection, the carbon-fiber microelectrode and optic fiber were positioned in thetelencephalon, in close proximity to each other (Figure 8), and the brain was perfused by oxygenated aCSF for 40 min. Upon stabilization of the background signal, 1000 ms light pulses were applied to quantify the photoelectric effect in brain tissue

responsible for the above discussed light artifact. A current of 0.52 $\pm$ 0.04 nA ($N = 3$) was recorded.

The uncaging of pHP-Glu was photochemically evoked after 30 min of brain perfusion with 1000 μM pHp-glutamate in aCSF. The light was applied with a duration of 1000 ms. Representative data documenting the successful uncaging process in whole brain and subsequent detection of 4HPAA are shown in Figure 8. A cyclic voltammogram sampled from the color plot at the time of light exposure (5 s) exhibits characteristics reflecting the oxidation of 4HPAA, including a prominent peak in current on the reverse scan at +1.24 V. The examination of the photoreleased current vs time plot (Figure 8, above color plot) shows a large increase in current at the time of light exposure. The measured current is significantly higher compared to the one recorded during light artifact measurement (Figure 9, one-way ANOVA with Tukey test, $p <$ 0.0001), and therefore, can be assigned primarily as a voltammetric response to the appearance of photoreleased 4HPAA.

We observed a prolonged current in the $I-t$ profile. It is possible that this current arises from adsorption of 4HPAA or another uncaging product to the electrode surface, resulting in either a faradaic current or alteration of the electrode double layer capacitance. Another contribution to this current might be slower diffusion of 4HPAA in the brain tissue. More work is
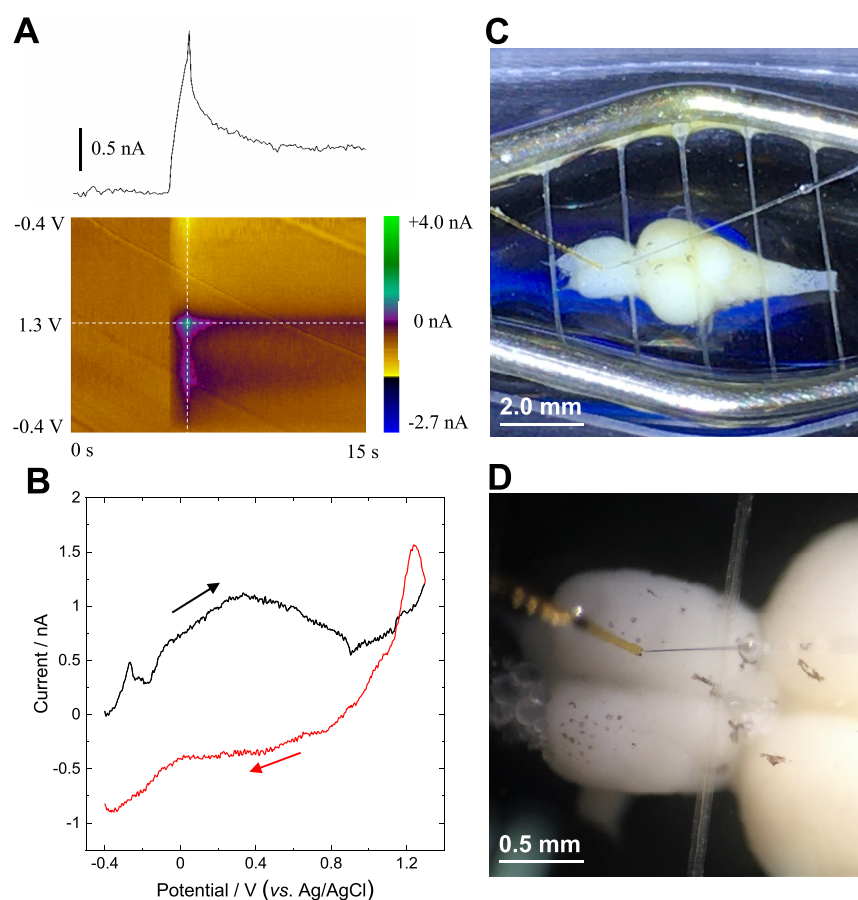
Figure 8. Representative data of 4HPAA detection in a zebrafish whole brain after pHp-glutamate photo-uncaging. Current vs time plot with corresponding color plot (A) and CV (B) are shown. pHP-Glu (1000 μM) in aCSF was perfused through the brain for 30 min. Direction of the potential sweep is indicated by arrows. Duration of light exposure: 1000 ms. The placement of the carbon-fiber working electrode and optic fiber in the telencephalon of a zebrafish brain (C, D).
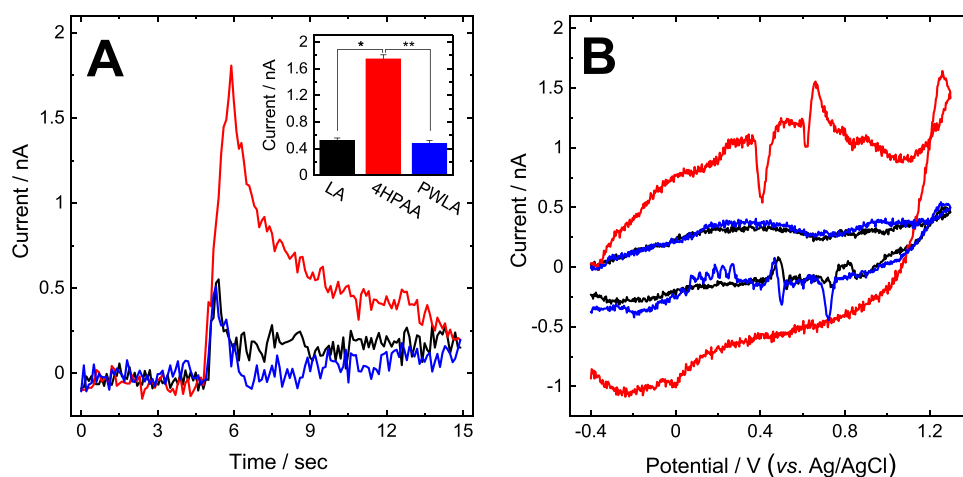

Figure 9. Representative current vs time (A) and CV (B) data for light artifact (LA) before the pHp glutamate administration (black), photoactivation of pHP Glu (red), and the light artifact recorded after 30 min post washout (post washout light artifact, PWLA) with pHp-Glu free aCSF (blue). Inset: photoinduced 4HPAA release measured after 30 min of pHp Glu perfusion through the brain was significantly increased in comparison with light artifact (*$p < 0.0001$, one way ANOVA, Tukey post hoc test, $N = 3$). The light artifact recorded after caged compound washout was significantly different from the 4HPAA measurement (**$p < 0.0001$), but not significantly different from the signal recorded before the caged compound administration ($p = 0.3462$). Duration of light exposure: 1000 ms.

needed to characterize each of these contributions. After subtraction of the photoinduced current, the resulting current was 1.23 ± 0.06 nA ($N = 3$ different electrodes and locations), which corresponds to formation of 21.1 ± 0.9 μM 4HPAA

(calculated from the concentration vs current plot, Figure 7C) and 22.2 ± 1.0 μM glutamate. A significantly lower signal was obtained for the experiments carried out in a whole brain in comparison with the one performed in the reaction vessel (for

the same exposure time of 1000 ms), suggesting lower uncaging power of the system in an opaque brain tissue. Despite this fact, we have successfully provided proof of concept for our newly developed method for the *in situ* monitoring of caged compound photochemistry. Importantly, the uncaging capacity is powerful enough to photorelease an amount of glutamate in excess of its estimated extracellular concentration range (0.02 to 20 μM).[37] Additionally, the amount of the photoreleased glutamate can be tailored based on individual needs, as the released concentration can be altered by the length of the uncaging time and light intensity.

Finally, to ensure that the recorded signal arises from the oxidation of 4HPAA, we conducted an experiment in which we applied a pulse of light to the zebrafish brain in the region where the electrode was located and measured the current response with FSCV. Prior to addition of *p*HP-Glu, a small artifactual current signal occurred that aligned with the light application. Upon application of *p*HP-Glu for 30 min, the magnitude of this light-induced signal increased several folds. After washing out *p*HP-Glu (and the products of the uncaging process) for at least 30 min, the signal returned to a level similar to that noted prior to adding *p*HP-Glu (Figure 9, one-way ANOVA with Tukey test, $p = 0.3462$, $N = 3$ different locations). These data indicate that the observed current arises from 4HPAA formation and possibly other electrochemically active species formed from the uncaging process and not simply the light artifact.

CONCLUSIONS

Our newly developed method can be used to quantify the degree of caged compound photolysis *in situ* with FSCV, a well-characterized electrochemical method. This approach is largely independent of the characteristics of the light source because light artifacts are subtracted out and the electrochemical signal is related directly to the concentration. Thus, our method depends only upon the electroactivity of the photoreleased cage, in this case, 4HPAA. Importantly, we have shown that 4HPAA, the product of photoreleased *p*HP-glutamate, can be easily detected and quantified in the telencephalon of a zebrafish whole brain. Thus, our work demonstrates the feasibility of photodelivering biologically active compounds in living tissues. In future studies, it will be important to validate this method in higher species such as mice and rats. This point is especially important since the brains in these species may have a more complex chemical makeup and opacity, resulting in problems such as increased electrode fouling or impairment of light access. Nevertheless, we expect this approach to have broad applicability, but it will be particularly well suited for cases that make quantitation of photons reaching the sample difficult, such as tissues or opaque liquids. Moreover, this method should also work when using caged compounds other than those based on *p*HP that release electroactive photocages, such as coumarins. Ultimately, adapting this method for *in vivo* application with a combined electrode, light guide, and caged compound delivery method will maximize its utility.

AUTHOR INFORMATION

Corresponding Author

Michael A. Johnson − *Department of Chemistry and R.N. Adams Institute for Bioanalytical Chemistry and Graduate Program in Neuroscience, University of Kansas, Lawrence, Kansas 66045, United States;* orcid.org/0000-0001-

5078-9896; Phone: 785-864-4269; Email: johnsonm@ku.edu

Authors

Romana Jarosova − *Department of Chemistry and R.N. Adams Institute for Bioanalytical Chemistry, University of Kansas, Lawrence, Kansas 66045, United States; Department of Analytical Chemistry, UNESCO Laboratory of Environmental Electrochemistry, Charles University, Prague 2 12843, Czech Republic*

Sam V. Kaplan − *Department of Chemistry and R.N. Adams Institute for Bioanalytical Chemistry, University of Kansas, Lawrence, Kansas 66045, United States*

Thomas M. Field − *Department of Chemistry and R.N. Adams Institute for Bioanalytical Chemistry, University of Kansas, Lawrence, Kansas 66045, United States;* orcid.org/0000-0002-9536-6317

Richard S. Givens − *Department of Chemistry and R.N. Adams Institute for Bioanalytical Chemistry, University of Kansas, Lawrence, Kansas 66045, United States*

Sanjeewa N. Senadheera − *Department of Pharmaceutical Chemistry, University of Kansas, Lawrence, Kansas 66045, United States*

Complete contact information is available at:
https://pubs.acs.org/10.1021/acs.analchem.0c03452

Author Contributions

M.A.J. conceived the work. This manuscript was written by M.A.J., S.V.K., R.J., and R.S.G. Experiments were carried out by R.J., M.A.J., S.V.K., and T.M.F. Compounds were synthesized by S.N.S. and the Synthetic Chemical Biology Core.

Notes

The authors declare no competing financial interest.

REFERENCES

(1) McCray, J. A.; Trentham, D. R. *Annu. Rev. Biophys. Biophys. Chem.* **1989**, *18*, 239−270.
(2) Adams, S. R.; Tsien, R. Y. *Annu. Rev. Physiol.* **1993**, *55*, 755−784.
(3) Ellis-Davies, G. C. R. *Nat. Methods* **2007**, *4*, 619−628.
(4) Ellis-Davies, G. C. R. *Beilstein J. Org. Chem.* **2013**, *9*, 64−73.
(5) Furuta, T. *J. Synth. Org. Chem., Jpn.* **2012**, *70*, 1164−1169.
(6) Corrie, J. E. T.; Furuta, T.; Givens, R. S.; Yousef, A. L.; Goeldner, M. Photoremovable Protecting Groups Used for the Caging of Biomolecules. *Dynamic Studies in Biology: Phototriggers, Photoswitches and Caged Biomolecules*; Wiley: 2005, 1−94, DOI: 10.1002/3527605592.ch1.
(7) Klán, P.; Šolomek, T.; Bochet, C. G.; Blanc, A.; Givens, R.; Rubina, M.; Popik, V.; Kostikov, A.; Wirz, J. *Chem. Rev.* **2013**, *113*, 119−191.

(8) Callaway, E. M.; Katz, L. C. *Proc. Natl. Acad. Sci. U. S. A.* **1993**, *90*, 7661−7665.

(9) Augustine, G. J. *J. Neurosci. Methods* **1994**, *54*, 163−169.

(10) Wang, S. S. H.; Augustine, G. J. *Neuron* **1995**, *15*, 755−760.

(11) Lipp, P.; Lüscher, C.; Niggli, E. *Cell Calcium* **1996**, *19*, 255−266.

(12) Hagen, V.; Frings, S.; Wiesner, B.; Helm, S.; Kaupp, U. B.; Bendig, J. *ChemBioChem* **2003**, *4*, 434−442.

(13) Bardhan, A.; Deiters, A. *Curr. Opin. Struct. Biol.* **2019**, *57*, 164−175.

(14) Gienger, M.; Hübner, H.; Löber, S.; König, B.; Gmeiner, P. *Sci. Rep.* **2020**, *10*, 829.

(15) Asad, N.; Mclain, D. E.; Condon, A. F.; Gore, S.; Hampton, S. E.; Vijay, S.; Williams, J. T.; Dore, T. M. *ACS Chem. Neurosci.* **2020**, *11*, 939−951.

(16) Hatchard, C. G.; Parker, C. A. *Proc. R. Soc. London, Ser. A* **1956**, *235*, 518−536.

(17) Heien, M. L. A. V.; Johnson, M. A.; Wightman, R. M. *Anal. Chem.* **2004**, *76*, 5697−5704.

(18) Troyer, K. P.; Wightman, R. M. *Anal. Chem.* **2002**, *74*, 5370−5375.

(19) Ortiz, A. N.; Kurth, B. J.; Osterhaus, G. L.; Johnson, M. A. *J. Neurochem.* **2010**, *112*, 755−761.

(20) Ortiz, A. N.; Oien, D. B.; Moskovitz, J.; Johnson, M. A. *Neuroscience* **2011**, *177*, 223−229.

(21) Maina, F. K.; Khalid, M.; Apawu, A. K.; Mathews, T. A. *J. Visualized Exp.* **2012**, *59*, 1−6.

(22) Kaplan, S. V.; Limbocker, R. A.; Gehringer, R. C.; Divis, J. L.; Osterhaus, G. L.; Newby, M. D.; Sofis, M. J.; Jarmolowicz, D. P.; Newman, B. D.; Mathews, T. A.; et al. *ACS Chem. Neurosci.* **2016**, *7*, 689−699.

(23) Johnson, M. A.; Rajan, V.; Miller, C. E.; Wightman, R. M. *J. Neurochem.* **2006**, *97*, 737−746.

(24) Johnson, M. A.; Villanueva, M.; Haynes, C. L.; Seipel, A. T.; Buhler, L. A.; Wightman, R. M. *J. Neurochem.* **2007**, *103*, 2102−2110.

(25) Kraft, J. C.; Osterhaus, G. L.; Ortiz, A. N.; Garris, P. A.; Johnson, M. A. *Neuroscience* **2009**, *161*, 940−949.

(26) Mohanaraj, S.; Wonnenberg, P.; Cohen, B.; Zhao, H.; Hartings, M. R.; Zou, S.; Fox, D. M.; Zestos, A. G. *J. Visualized Exp.* **2019**, *2019*, No. e59552.

(27) Smith, A. R.; Garris, P. A.; Casto, J. M. *J. Chem. Neuroanat.* **2015**, *66-67*, 28−39.

(28) Weisz, C. J. C.; Rubio, M. E.; Givens, R. S.; Kandler, K. *J. Neurosci.* **2016**, *36*, 911−925.

(29) Goeldner, M.; Givens, R. S. *Dynamic Studies in Biology: Phototriggers, Photoswitches and Caged Biomolecules*; Wiley: 2005, 1−557.

(30) Shin, M.; Kaplan, S. V.; Raider, K. D.; Johnson, M. A. *Analyst* **2015**, *140*, 3039−3047.

(31) Kandler, K.; Nguyen, T.; Noh, J.; Givens, R. S. *Cold Spring Harb. Protoc.* **2013**, *2013*, 118−121.

(32) Shin, M.; Field, T. M.; Stucky, C. S.; Furgurson, M. N.; Johnson, M. A. *ACS Chem. Neurosci.* **2017**, *8*, 1880−1888.

(33) Barker, G. C.; Gardner, A. W.; Sammon, D. C. *J. Electrochem. Soc.* **1966**, *113*, 1182.

(34) Barazzouk, S.; Hotchandani, S.; Vinodgopal, K.; Kamat, P. V. *J. Phys. Chem. B* **2004**, *108*, 17015−17018.

(35) Givens, R. S.; Weber, J. F. W.; Conrad, P. G.; Orosz, G.; Donahue, S. L.; Thayer, S. A. *J. Am. Chem. Soc.* **2000**, *122*, 2687−2697.

(36) Givens, R. S.; Stensrud, K.; Conrad, P. G.; Yousef, A. L.; Perera, C.; Senadheera, S. N.; Heger, D.; Wirz, J. *Can. J. Chem.* **2011**, *89*, 364−384.

(37) Moussawi, K.; Riegel, A.; Nair, S.; Kalivas, P. W. *Front. Syst. Neurosci.* **2011**, *5*, 94.